Primate Upper Limb Muscles Exhibit Activity Patterns That Differ From Their Anatomical Action During a Postural Task

Isaac Kurtzer, J. Andrew Pruszynski, Troy M. Herter, and Stephen H. Scott
Department of Anatomy and Cell Biology, Canadian Institute of Health Research Group in Sensory-Motor Systems,
Center for Neuroscience Studies, Queen's University, Kingston, Canada

Kurtzer, Isaac, J. Andrew Pruszynski, Troy M. Herter, and Stephen H. Scott. Primate upper limb muscles exhibit activity patterns that differ from their anatomical action during a postural task. *J Neurophysiol* 95: 493–504, 2006. First published October 26, 2005; doi:10.1152/jn.00706.2005. The present study examined muscular activity in the primate proximal forelimb during a posture task. By applying loads selectively to the shoulder, elbow, or both joints, we observed that monoarticular shoulder and elbow muscles varied their activity with loads at the unspanned joint. Shoulder monoarticulars changed activity with elbow torque and elbow monoarticulars changed activity with shoulder torque. Due to this additional modulation, the maximal activation of monoarticular muscles was deviated from their anatomical action toward either shoulder-extension/elbow-flexion or shoulder-flexion/elbow-extension. Biarticular muscles also expressed deviations in their preferred torque direction toward either shoulder-extension/elbow-flexion or shoulder-flexion/elbow-extension. The biased distribution of preferred torque directions in proximal forelimb muscles could be modeled by the minimization of a global measure of muscle activity. Moreover, arm-related neurons of primary motor cortex exhibit a similar bias in preferred torque directions consistent with the intimate relationship between the primary motor cortex and the motor periphery.

INTRODUCTION

The primate proximal forelimb possesses muscles that cross multiple joints and joints that are crossed by multiple muscles. This redundant musculature allows identical motor actions to be achieved with different patterns of muscle activation. Consequently, determining how the nervous system adopts a particular pattern of muscle activity is a prominent question in motor control research (Buchanan et al. 1986, 1989; Crowninshield and Brand 1981; Dul et al. 1984; Jongen et al. 1989a; Penrod et al. 1974).

In the present paper, we examined tonic changes in muscular activity associated with changes in muscular torque, i.e., torque-related activity. Recordings were obtained from the primate proximal forelimb during a posture task. We were particularly interested in whether the muscles' maximal activity was aligned with their anatomical action or whether the muscles expressed a "preferred torque direction" (PTD) different from their anatomical action.

Deviation in a muscle's PTD from its anatomical action (PTD rotation) has been previously reported for the monkey wrist (Hoffman and Strick 1999), human leg (Nozaki et al. 2005), and the human arm during wrist supination and elbow torques (Buchanan et al. 1989; van Zuylen et al. 1988). In these studies, ". . . the activation of a single muscle cannot be understood solely from the anatomy of this single muscle and from its tendon insertion and origin" (van Zuylen et al. 1988; p. 1524). For example, when gluteus maximus helps resist an applied force at the ankle, its maximal activation occurs with a combination of hip extension and knee extension torque (Nozaki et al. 2005). Its multi-joint PTD is initially surprising because gluteus maximus is a monoarticular hip extensor and does not contribute any torque at the knee. However, PTD rotations will occur when muscular recruitment is based on a global strategy of minimizing the total muscular activity or effects of motor noise (Fagg et al. 2002; Nozaki et al. 2005). This strategy favors low levels of muscle activity where the muscles have similar mechanical actions and higher levels where fewer muscles can contribute. Thereby, the muscles' PTDs tend to rotate to the gaps in torque space with few or no muscles.

Biarticular muscles in the primate proximal forelimb generate either extension (long head of the triceps, dorsoepitrochlearis) of both shoulder and elbow joints or flexion (short and long heads of the biceps) of both joints. This arrangement creates two prominent gaps in the shoulder-elbow torque space as there are no muscles that create shoulder-flexion/elbow-extension (SE/EF) or shoulder-extension/elbow-flexion (SF/EE) torques. If the nervous system recruited shoulder and elbow muscles through a strategy of minimizing the total muscular activity, then we would expect a rotation of the monoarticulars' PTDs toward these gaps in torque space.

In the present study, we examined the direction tuning of proximal limb muscles by selectively applying mechanical loads to the shoulder, elbow, or both joints together. Although PTD rotations are apparent in some studies using elbow and shoulder torques (Osu and Gomi 1999; Soechting and Lacquaniti 1988; van Bolhuis and Gielen 1999), we have added to these observations by quantifying the extent of PTD rotation in the monkey's upper limb. Further, by varying the load at a single joint for a fixed level of torque at the other joint (Scott 1999), we could unambiguously identify monoarticular activity linked to loads at the unspanned joint.

An additional motivation for this study was to compare the torque-related activity of proximal forelimb muscles with the torque-related activity of primary motor cortex neurons in the same task. More than a century of research has indicated primary motor cortex (M1) is the principal cortical site for voluntary motor execution, particularly for primates (Canedo

---

1997; Hepp-Reymond 1988; Porter and Lemon 1993; Scott 2003). In a previous study, we reported a population bias of M1 neurons in responding to elbow and/or shoulder torques (Cabel et al. 2001). Most neurons discharged maximally with a combination of SE/EF or SF/EE torques compared with extension/extension or flexion/flexion torques. Here we test whether the muscles of the proximal forelimb exhibit a similar bias toward SE/EF and SF/EE.

Our results indicate that proximal forelimb muscles of the monkey—including shoulder monoarticular, elbow monoarticular, and biarticular muscles—typically exhibit PTD rotations toward SE/EF and SF/EE torques, as observed in M1, and similar to models that minimize the total muscular activity. Preliminary experimental observations have been previously published (Cabel et al. 2001).

METHODS

Task and apparatus

We examined the muscular activity of four male rhesus monkeys (*Macaca mulatta*, 6–12 kg) trained to perform forelimb motor tasks with the KINARM device (Scott 1999). KINARM is a robotic exoskeleton that supports the limb, allows planar shoulder and elbow motion, monitors those joint motions, and can apply mechanical loads to the shoulder and/or elbow joints independently. This apparatus was coupled with a virtual-reality system that permitted the monkey to view its entire limb and visual targets in the horizontal plane of movement. All procedures followed guidelines set by the Queen's University Animal Care Committee.

Monkeys performed a postural task as described in a previous study (Cabel et al. 2001). Each monkey maintained its right hand within a 0.8-cm-wide circular target near the center of the limb's workspace where the shoulder and elbow passive torques were minimal (Graham et al. 2003). Postural maintenance occurred for 3–4 s while constant flexion or extension loads were applied at the shoulder, elbow, both, or neither joint (Fig. 1A). Consequently, nine load conditions were employed: four single-joint, four multi-joint, and one no-load baseline condition. The constant load magnitude was ±0.12 Nm for *monkeys A–C* and ±0.32 Nm for the largest monkey, *D*. The nine load conditions were presented in a pseudorandom block design repeated five times. We examined the final 2 s of this period after which any small stabilizing movements had ended (Fig. 1B).

Muscle recording

Acute and chronic techniques were used to record electromyographic (EMG) activity using standard recording techniques (Loeb and Gans 1986; Scott and Kalaska 1997). Acute recordings were obtained from all monkeys by percutaneously inserting single-strand wires and micro-stimulating the muscle to verify the electrode placement. Chronic recordings were obtained from *monkeys A and C* after surgical implantation of bipolar multi-strand electrodes in the superficial portion of the muscle belly. For both techniques, the EMG signals were sampled at 1,000 Hz for *monkey A* and at 4,000 Hz for *monkeys B–D,* full-wave rectified, and then integrated into 5-ms bins.

We recorded activity of 12 different proximal forelimb muscles with a principal action for shoulder-elbow extension/flexion, see Table 1. Several of these muscles were sampled from different monkeys or the same monkey with different recording techniques (acute and chronic) for a total of 34 samples. Muscles were selected if they exhibited directionally tuned responses during unloaded reaching movements ($P < 0.01$, plate method) (Gribble and Scott 2002) and received a score ≥ 3 from a subjective rating of signal quality between 1 (poor) and 5 (excellent).

Data analysis

We were primarily interested in examining changes in muscular activity associated with changes in muscular torque, i.e., torque-related activity. Change in muscle activity was quantified by the difference in mean rectified voltage between the loaded and unloaded conditions. Likewise, the change in muscle torque was measured between the loaded and unloaded conditions and was opposite to the imposed load (Scott 1999); note that the limb's stable posture ensured that muscle torque reflected compensations to the imposed load rather than limb dynamics. As we subtracted baseline, both the muscle activity and muscle torque could exhibit positive and negative values.

Torque-related muscular activity was assessed by measures of the preferred torque direction (the relative sensitivity to shoulder and elbow torques) and torque gain (the absolute sensitivity to shoulder and elbow torques). Planar-fits of the torque-related activity yielded shoulder (S) and elbow (E) coefficients used to calculate the preferred torque direction—atan(E/S) — and the torque gain—$(E^2 + S^2)^{1/2}$ (Kurtzer et al. 2005). Preferred torque direction was measured counter-clockwise from shoulder flexion so shoulder flexor, elbow flexor, shoulder extensor, and elbow extensor response directions occurred at 0, 90, 180, and 270°, respectively (Fig. 1A).

The inter-trial reliability of a muscle's PTD was assessed by separate plane fits to each of the five repeat blocks, nine load conditions each time, to yield five PTDs. The five repeat PTDs (unit length = 1) were added tip-to-tail and normalized by their absolute length for a mean vector the length of which ranges from 0 to 1 for perfectly random (0) to perfectly similar (1) response directions. The mean vector length was transformed into an angular SD and 99% angular confidence interval about the measured PTD (Batschelet
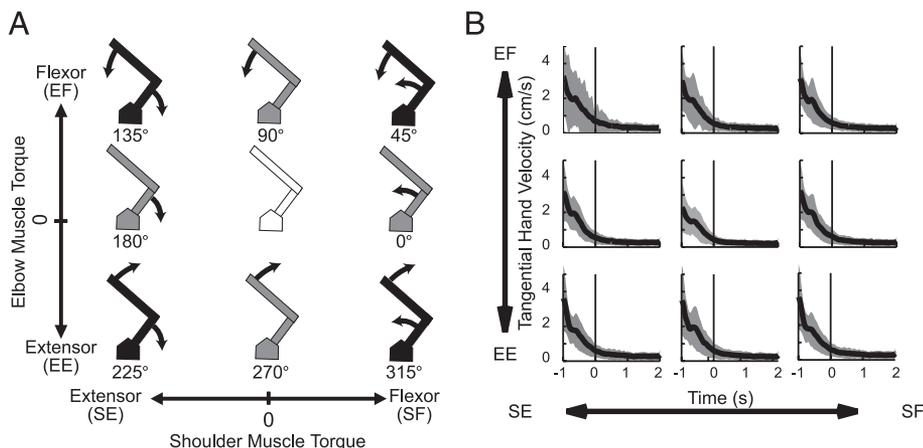

FIG. 1. Experimental setup. *A*: coordinate frame of muscle torques required for the 9 load conditions. Shoulder torque is represented along the *x* axis and elbow torque is represented along the *y* axis; flexion torque is positive and extension torque is negative. Of the 9 load conditions, there are 4 single-joint conditions (denoted by gray shading), 4 multi-joint conditions (denoted by black shading), and 1 is a no-load baseline condition at the center (denoted by white shading). Angles are in degrees and counter-clockwise order. *B*: temporal changes in tangential hand velocity observed in each condition. Mean (black lines) and SD (gray shading) are calculated from the mean tangential hand velocity observed in 251 task repeats. Vertical line indicates onset of 2-s window when the data were analyzed.

TABLE 1. *Muscles samples*

Muscle Group	Muscle-expected PTD	Samples*-measured PTD
Shoulder extensor	Posterior deltoid-180° (DP)	Chronic: A PTD: 148° ± 3°; R^2 = .55 C PTD: 148° ± 12°; R^2 = .87 Acute: C PTD: 147° ± 6°; R^2 = .60
Shoulder flexor	Anterior deltoid-0° (DA)	Chronic: A PTD: 0° ± 6°; R^2 = .84 C PTD: 327° ± 6°; R^2 = .64 Acute: C PTD: 327° ± 7°; R^2 = .62
	Pectoralis major-0° (PM)	Chronic: C PTD: 348° ± 6°; R^2 = .65 Acute: B PTD: 2° ± 17°; R^2 = .64 C PTD: 336° ± 7°; R^2 = .76 D PTD: 27° ± 4°; R^2 = .60
Elbow extensor	Triceps lateral-270° (Tla)	Acute: B PTD: 293° ± 18°; R^2 = .59 D PTD: 298° ± 13°; R^2 = .53
	Triceps medial-270° (Tme)	Acute: A ns B PTD: 296° ± 6°; R^2 = .70
Elbow flexor	Brachialis-90° (B)	Chronic: A PTD: 125° ± 1°; R^2 = .53 C PTD: 121° ± 10°; R^2 = .60 Acute: A ns B PTD: 120° ± 4°; R^2 = .63 C PTD: 114° ± 6°; R^2 = .69 D PTD: 114° ± 10°; R^2 = .56
	Brachioradialis-90° (Br)	Chronic: C PTD: 115° ± 18°; R^2 = .64 Acute: B PTD: 111° ± 3°; R^2 = .85 D PTD: 96° ± 7°; R^2 = .77
Biarticular extensor	Extensor carpi radialis longus-90° (ECRL) Triceps long-198° (Tlo)	Acute: D PTD: 102° ± 10°; R^2 = .67 Chronic: A PTD: 150° ± 3°; R^2 = .72 C PTD: 144° ± 6°; R^2 = .85 Acute: A ns B PTD: 150° ± 11°; R^2 = .61
Biarticular flexor	Dorsoepitroclearis-209° (De) Biceps long-71° (BL)	Acute: D PTD: 152° ± 5°; R^2 = .76 Acute: B PTD: 110° ± 15°; R^2 = .36 D PTD: 70° ± 38°; R^2 = .24
	Biceps short-51° (BS)	Chronic: A ns Acute: B PTD: 80° ± 8°; R^2 = .62 D PTD: 71° ± 25°; R^2 = .29

1981). If the anatomical action was outside the confidence interval, the measured muscle PTD was considered significantly rotated.

We also utilized a complimentary parameter-free descriptive model, the plate method (Gribble and Scott 2002), which characterized the "mass distribution" of EMG activity across torque direction without assuming an underlying tuning function. The orientation of the mass center is related to the preferred torque direction and its magnitude is related to the torque gain. The plate method characterized the specificity of the muscle's response to load conditions (i.e., tuning width) with a "ratio of inertia" score (IR) ranging from 0 to 1 for a maximally sharp to uniform response (Gribble and Scott 2002). Note that we looked specifically at torque-related activity by first subtracting baseline activity from the no-load condition and then shifting the data by the lowest value to create all positive values; this has the effect of narrowing the tuning width. An untruncated cosine function, i.e., equal amount of change above and below baseline, has an IR = 0.44 and a truncated cosine has an IR < 0.44.

We employed several additional statistics in examining the patterns of muscular activity. First, two-way ANOVAs tested for main effects of shoulder and/or elbow torques within a muscle (3 levels for shoulder and elbow). Second, χ^2 tests identified any trend in PTD rotation (significant deviation toward SE/EF or SF/EE, away, or no significant rotation. Third, a Rayleigh's test determined if the entire sample of PTDs was significantly bimodal (Baschelet 1981). And fourth, a circular bootstrap test assessed similarity of two groups of PTDs (e.g., from single joint-joint and multi-joint load conditions) by comparing the circular correlation of their observed pairing with that from a random pairing (4,000 repeats). A consistently larger circular correlation for the observed pairing than the random pairing indicates

a systematic similarity between the observed PTD pairs. All statistical tests were considered significant at $P < 0.01$.

Model of muscle activation

We tested whether the observed rotation of muscle activation (see RESULTS) could result from minimizing various global features of muscular activity: muscle force, muscle metabolic energy, and muscle noise. Each minimizing model utilized a lumped representation for the six muscle groups—shoulder extensor, shoulder flexor, elbow extensor, elbow flexor, biarticular flexor, biarticular extensor—using known values for the monkey moment arms, fascicle length (l) and physiological cross-sectional areas (PCSA) (Cheng and Scott 2000; Graham and Scott 2003). All models were further constrained so that muscles could only pull, conditions were isometric, and muscle parameters were constant; activation per unit torque is inversely proportional to a muscle's moment arm.

An iterative procedure scaled each muscle group's activity to achieve a target torque with the minimal summed force ([sumn]f'') (Penrod et al. 1974), metabolic energy [[sumn] $(f_i*l_i)^n$] (Happee 1992), or muscle noise [[sumn]$(f_i*/PCSA_i)^n$] (Hamilton et al. 2004; Harris and Wolpert 1998; van Bolhuis and Gielen 1999) raised to a power n from 1 to 3; note that this model of muscle noise is equivalent to muscle stress (van Bolhuis and Gielen 1999). The parameter n varies each muscle's cost term from linear to cubic. Minimization was achieved with the Matlab function (fmincon) which finds a minimum of a constrained nonlinear function (The Mathworks, Natick, MA). To avoid local minima we repeated this procedure 100 times from random initializations and selected the lowest value. The resulting

optimal activation of each modeled muscle was plotted across target torques and summarized by the PTD (see *Data analysis*).

RESULTS

General features of activity

During the postural task, monkeys maintained their hand position near the center of the workspace while countering a constant torque applied to the shoulder and/or elbow joints. This arrangement is summarized in the muscle-torque coordinate frame of Fig. 1*A*. After a brief period of stabilization the monkeys achieved a nearly stationary posture within the small target window. This is evident in the low hand velocity during the final 2 s, Fig. 1*B*. Mean hand velocity in this interval was typically <0.5 cm/s, <5% of the peak velocity during reaching movements. The nearly stationary conditions allowed compensatory changes in muscular activity to be specifically related to countering the imposed loads rather than the limb's dynamics.

Of the 34 muscle samples, 32 (~94%) expressed significant changes in activity related to compensatory shoulder or elbow muscular torques (2-way ANOVA, $P < 0.01$). Planar regressions were also typically significant (30/34, 88%, $P < 0.01$) and accounted for a high percentage of the torque-related variance ($r^2 = 0.63 \pm 0.15$, mean $\pm$ SD; Fig. 2, *A* and *B,* and Table 1). All 12 muscle types included significant samples and the few nonsignificant samples did not arise from a single muscle type. The following analyses focuses on those muscle samples with significant plane fits.

Muscles flagged by the plane-fits exhibited highly similar responses to single- and multi-joint load conditions. Eight-two percent of the cases had significant plane fits to both the single- and multi-joint loads taken separately ($P < 0.01$). For this subset, the intra-muscle PTDs were highly similar between single- and multi-joint load conditions ($P < 0.01$, circular bootstrap); the absolute angular difference was ~17.6° on average (Fig. 3*A*). Likewise, the torque gains between single- and multi-joint load conditions were highly similar ($r = 0.87$, $P < 0.01$; Fig. 3*B*). For example, the brachioradialis in Fig. 2*A* had a 17° difference in PTD and a 3% difference in torque gain between the single- and multi-joint load conditions.

The sampled muscles also had larger activity increases from baseline than decreases from baseline along their PTD-axis (Figs. 4*A* and 6). This feature has been observed in previous studies where the limb was supported against gravity (Hoffman and Strick 1999; Nozaki et al. 2005; Theeuwen et al. 1994). Gain values were approximately eight times larger for the activity increases than decreases (7.9 $\pm$ 16, plane fit) although both increases (97%) and decreases (83%) were usually flagged as significant ($P < 0.01$).

The inequality between activity increases and decreases meant that the sampled muscles exhibited relatively sharp tuning widths. An idealized muscle tuned to just one load condition would be maximally sharp and have an IR approaching zero. The present sample did not reach this limit but was typically more sharp than an untruncated cosine (IR = 0.27 $\pm$ 0.15, SD < cosine = 0.44; *t*-test, $P < 0.01$; Fig. 4*B*). It should be noted there was considerable variability in tuning width across samples and that no significant differences in tuning width were observed between muscle groups (1 × 6 ANOVA, $P > 0.05$).

The previous comparisons between single- and multi-joint responses and between torque-related increases and decreases were obtained with the planar regression. However, similar
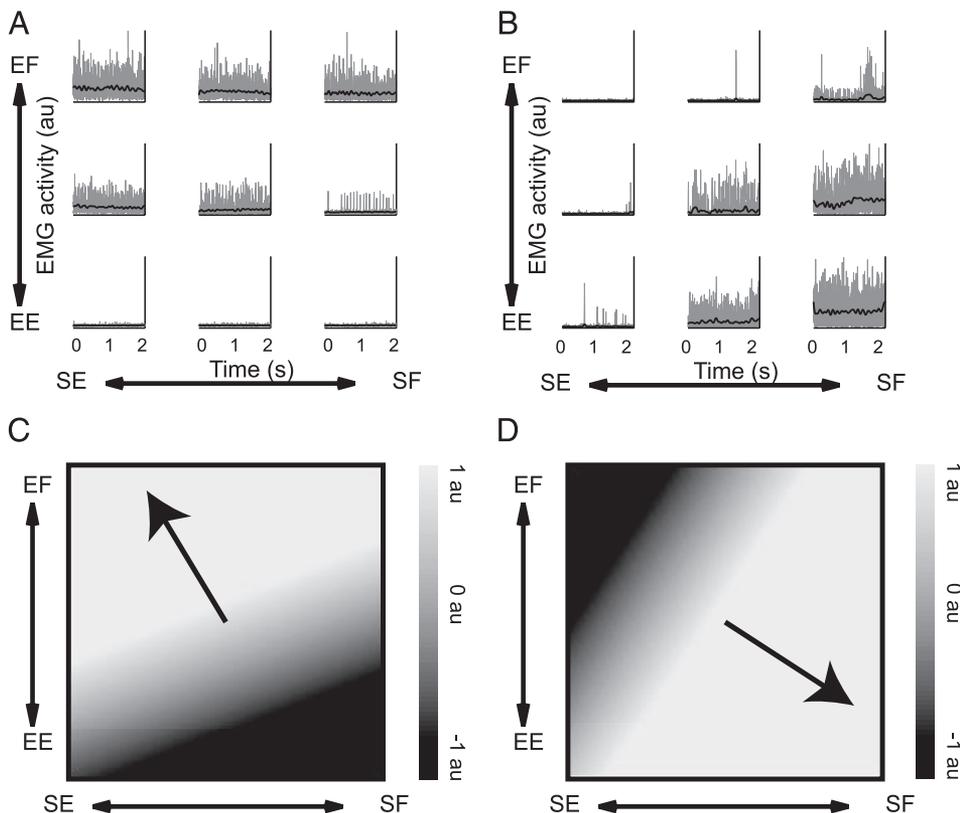

FIG. 2. Two exemplar monoarticular muscles. *A* and *B*: raw electromyographic (EMG) activity of brachioradialis (elbow flexor, session acute B) and anterior deltoid (shoulder flexor, chronic C) presented in the joint-torque coordinate frame of Fig. 1*A*. Mean activity (black lines) after filtering (6th-order Butterworth with a 10-Hz low-pass cutoff) is superimposed on the unfiltered activity of the individual trials (gray lines). Activity is in arbitrary scaled units (au). *C* and *D*: surface plots of the plane-fit regressions from the preceding exemplar muscles. Gradients indicate increases (white) and decreases (black) from baseline. Arrows indicate the preferred torque directions for the sampled brachioradialis (anatomical = 90° vs. measured = 111 $\pm$ 3°) and anterior deltoid (anatomical = 0° vs. measured = 327 $\pm$ 7°).
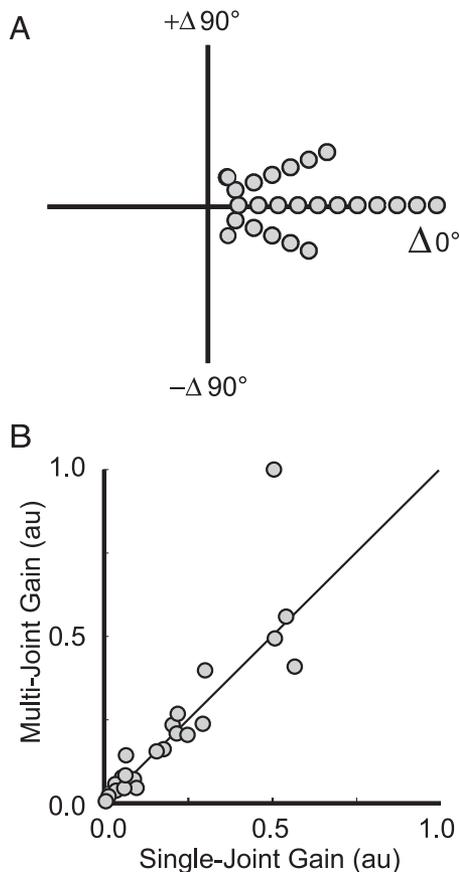
FIG. 3. Tuning properties of EMG activity during single- vs. multi-joint torques. *A*: polar histogram of changes in preferred torque direction (PTD) between single- and multi-joint load conditions (single-joint PTD–multi-joint PTD) for each muscle sample; single- and multi-joint PTDs were determined from separate plane fits ($P < 0.01$) carried out on the single- and multi-joint load conditions. *B*: comparison of the single- and multi-joint torque gains for each muscle sample using the same separate plane fits used in *A*. Activity is in arbitrary scaled units of voltage (au).

observations were apparent with the parameter-free plate method.

Deviations of PTD from the anatomical action

The principal concern of this study was to determine whether muscles of the primate proximal forelimb exhibit PTDs that are systematically deviated from their anatomical action. In fact, such deviations were typical. Figure 2*A* depicts this property for a single-joint elbow flexor, brachioradialis. Because this muscle spans the elbow joint we expected muscular activity to change with elbow muscle torque. Appropriate activity changes were observed via an increase from baseline with elbow flexor torque and a decrease from baseline with elbow extensor torque. Importantly, activity was also modulated by loads at the shoulder joint for a fixed level of elbow torque—increases with shoulder extensor torque and decreases with shoulder flexor torque. A two-way ANOVA confirmed that this muscle was modulated by both shoulder and elbow torques ($P < 0.01$). Also the 99% angular confidence interval of the planar regression indicated that its PTD was significantly rotated toward shoulder extension (anatomical = 90°, measured = 111 ± 3°; Fig. 2*C*). Therefore this single-joint elbow

muscle exhibited multi-joint behavior related to both the elbow and shoulder.

A session from another single-joint muscle, anterior deltoid, is shown in Fig. 2*B*. As expected, this shoulder flexor exhibited increased activity with shoulder flexor torque and decreased activity with shoulder extensor torque. Moreover, activity increased with elbow extensor torque and decreased with elbow flexor torque. The 2 × 2 ANOVA and angular confidence interval confirmed that this muscle was significantly modulated by torques at both joints ($P < 0.01$) and its PTD was significantly rotated toward elbow extension (anatomical = 0°, measured = 327 ± 7°; Fig. 2*D*).
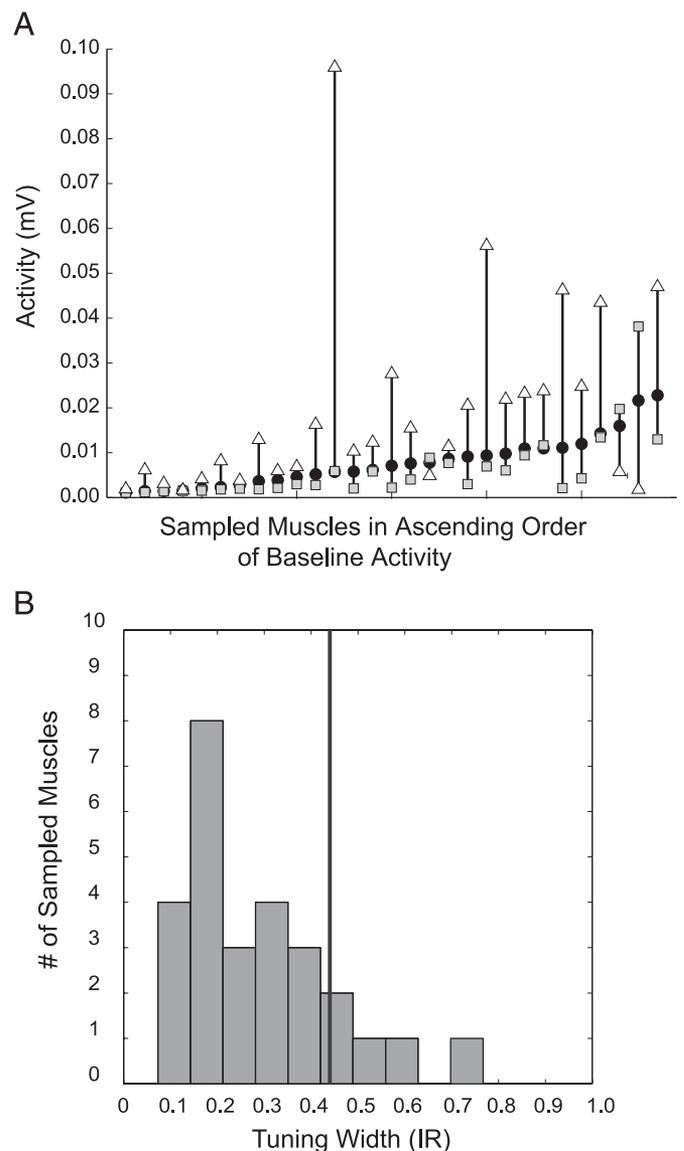

FIG. 4. Additional tuning properties of EMG activity. *A*: comparison of baseline activity (circle) with activity at the torque condition nearest the PTD (symbol above each circle) and activity at the torque condition opposite the PTD (symbol below each circle) for each muscle sample with a significant plane fit ($P < 0.01$). Muscle samples are organized according to their baseline activity (lowest to highest). Triangles indicate the larger change from baseline. Squares indicate the smaller change from baseline. Scale is in mV. *B*: population histogram of tuning widths (IR) for all muscle samples. IR of untruncated cosine = 0.44.
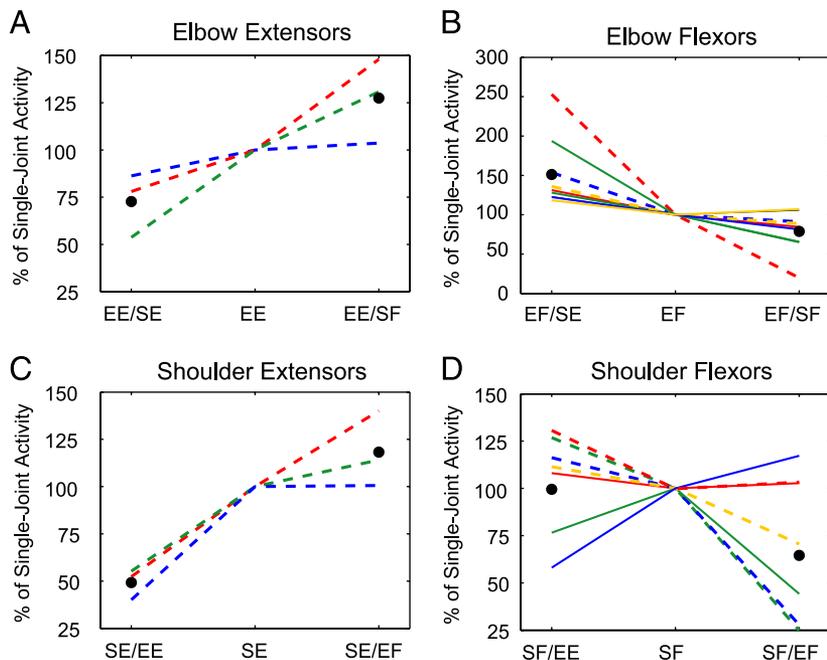
FIG. 5. Monoarticular EMG activity during muscular torque at the unspanned joint. *A–D*: mean activity for each monoarticular muscle sample during a fixed level of muscle torque at the principal joint paired with flexor, extensor, or no torque at the unspanned joint. Activities during flexor and extensor torques at the unspanned joint are normalized to the single-joint condition with no torque at the unspanned joint. Each colored line per panel indicates a different muscle sample with a significant plane fit. Thick dots are the group means.

We consistently observed modulations in activity when a muscle produced torque along its anatomical action coupled with torques at the unspanned joint. Figure 5, *A–D,* depicts this secondary modulation for the four monoarticular groups. During elbow extension, the elbow extensors showed 27% less activity with shoulder extensor torque and 23% more activity with shoulder flexor torque. Similarly, elbow flexors showed 21% less activity when elbow flexion was paired with shoulder flexor torque and 50% more activity when paired with shoulder extensor torque. Shoulder muscles exhibited a complimentary pattern. Shoulder extensor activity decreased by 51% and increased by 18% with elbow extensor and flexor torque. Last, shoulder flexor activity decreased by 35% with elbow flexor torque but only increased by 4% with elbow extensor torque.

t-test compared these differences in activity during flexion and torques at the unspanned joint of a muscle when that muscle produced torque along its anatomical action ($P < 0.01$). As a group, monoarticular elbow flexors, elbow extensors, and shoulder extensors all showed significant trends, but monoarticular shoulder flexors showed only a weak trend due to their high variability ($P < 0.10$). In a complementary analysis, two-way ANOVAs flagged 73% of the individual monoarticulars for significant changes in activity due to torques at both joints ($P < 0.01$).

Plane-fit regressions using responses to all the load conditions revealed rotated PTDs in all muscle groups—single-joint shoulder flexors/extensors, single-joint elbow flexors/extensors, and biarticular flexors/extensors. One sample from each muscle group is depicted in Fig. 6. Each panel shows the muscle's activity, anatomical action, and PTDs of its individual trials in joint-torque coordinates. Here the PTD rotations ranged from 21 to 48° with 99% confidence intervals outside 0° indicating a significant rotation from anatomical action.

The examples reflect a general trend where each muscle group had a mean PTD rotation toward SE/EF or SF/EE (Fig. 7, *A–C*). Single-joint elbow flexors (extensors) expressed 23 ± 12° (25 ± 2°) of PTD rotation. Single-joint shoulder flexors (extensors) expressed PTD-rotations of 10 ± 28° (32 ± 1°;
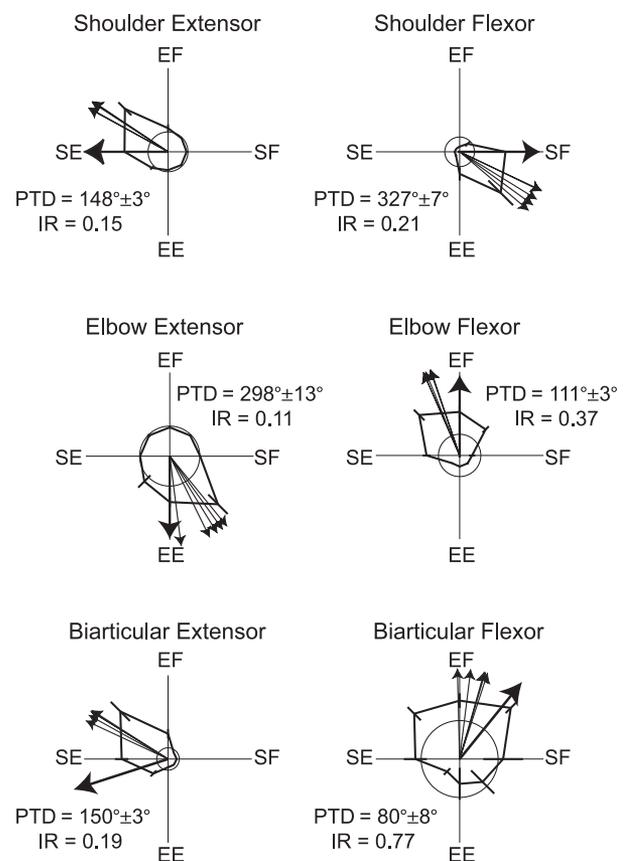

FIG. 6. Mean EMG activity in joint-torque coordinates for exemplar monoarticular and biarticular muscles. One exemplar muscle sample is depicted for each of the 6 muscle groups: shoulder extensor (chronic A-posterior deltoid), shoulder flexor (acute C-anterior deltoid, elbow extensor (acute D-triceps lateral), elbow flexor (acute B-brachioradialis), biarticular extensor (chronic A-triceps long), and biarticular flexor (acute B-biceps short). Mean activities (±SD) are shown for the 8 load conditions (black lines) together with the mean activity in the no-load baseline condition (black circle). Small arrows indicate the PTD for each of the 5 repeat blocks (see METHODS), and large arrows indicate the anatomical action. Mean PTDs (±95% confidence interval) and IR are indicated in panels.
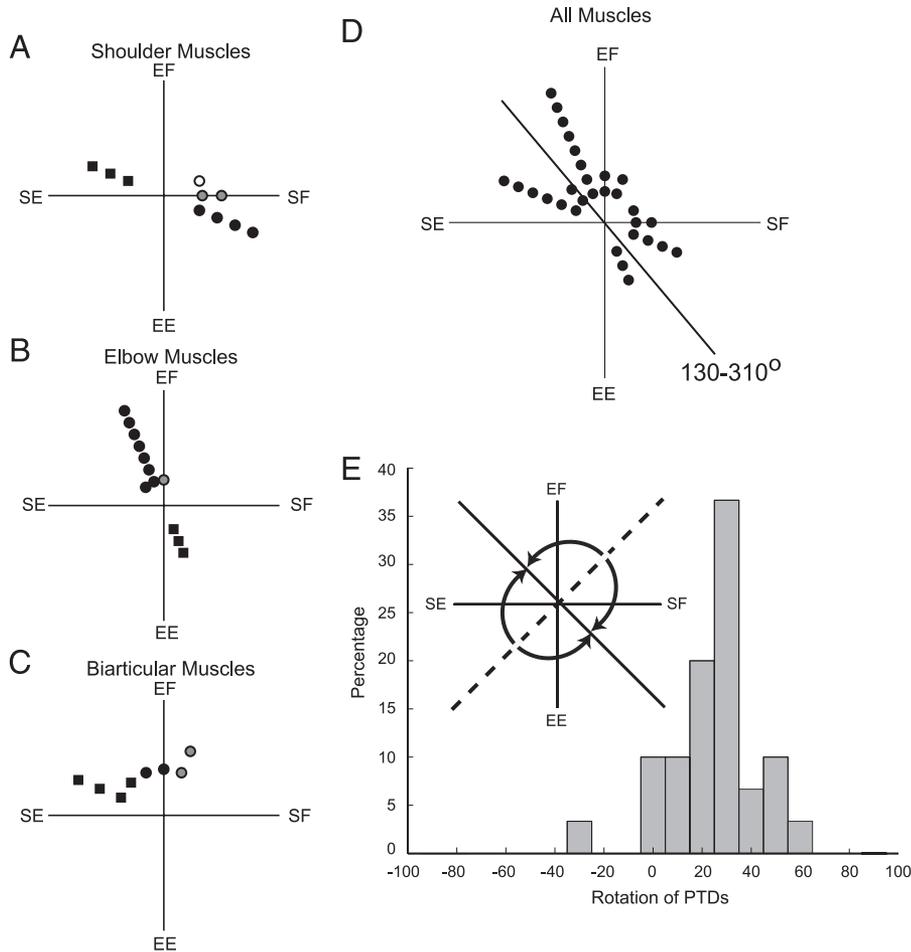
FIG. 7. Distribution of PTDs across all muscle samples. *A–D*: polar histograms of the PTDs in joint-torque coordinates are depicted for shoulder, elbow, biarticular, and all muscle samples, respectively. In *A–C,* the squares signify extensors, and the circles signify flexors. ● and ■ denote significant rotation toward shoulder-extension/elbow flexion (SE/EF) or shoulder-flexion/elbow extension (SF/EE); ○, a significant rotation away from these directions; and ◒, no significant rotation (see *inset* in *E*). *D*: all samples are presented as ●. —, the axis of the bimodal distribution. *E*: population histogram of PTD rotations toward (positive) and away (negative) from SE/EF or SF/EE. The width of each bar is 10°. *Inset*: Definition of direction of PTD rotation. Depending on where a muscle has a mechanical action (→) then a clockwise or counter-clockwise rotation of its PTD would approach the quadrant of SE/EF or SF/EE.

mean ± SD). And the biarticular flexors (extensors) expressed PTD rotations of 22 ± 20° (52 ± 5°). Across all the sampled muscles the mean PTD rotation (25 ± 24°) was significantly different from zero ($P < 0.01$, Fig. 7*E*). A χ^2 test using categorical possibilities of rotation—significant rotation toward SE/EF or SF/EE, away, or none—confirmed this bias across the set of sampled muscles ($\chi^2 = 30.2$, $P < 0.001$, Fig. 7*E*). Consequently, the entire sample of PTDs was not significantly different from a bimodal distribution clustered about an axis at 130–310° (Rayleigh test, $R_c = 0.54$). This is nearly orthogonal to the distribution one would expect if the muscles' PTDs were aligned with their anatomical action, 50–230°. Similar results were obtained with alternative tests of directionality; the mean absolute angular difference between the planar regression and vector methods (Baschelet 1981) was 4.6° and between the planar regression and plate methods (Gribble and Scott 2002) was 3.5°.

The preceding results indicate a consistent trend for PTD rotation of shoulder and elbow muscles toward SE/EF or SF/EE. However, there was also considerable variability in the amount of rotation, Table 1; the SD of PTD rotations across all muscle samples is 24° (Fig. 8, *A*). To address the sources of this variability, we calculated the angular SD associated with five different factors: the monkeys, muscle groups, mechanical action, recording type, and session (Fig. 8, *B–F*). Monkeys expressed similar PTD rotations on average compared with the average variability within each monkey (8.5 vs. 24° SD, Fig. 8, *B*). Substantial variability was also present at the level of

muscle groups, but flexors tended to have larger and more variable PTD rotations (see Table 1). The average variability among the six groups was 11.5° SD (Fig. 8, *C*).

Less variability was evident when we examined specific muscle groups and monkeys together. The mean variability was 7.5° SD among muscles having a similar mechanical action and sampled from the same monkey (e.g., brachioradia-
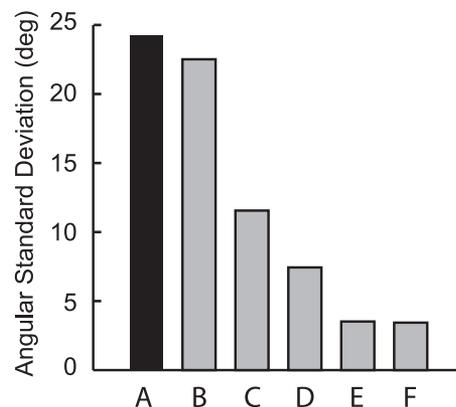

FIG. 8. Variability of PTD rotations. Each column depicts the angular SD of muscle samples. A: SD across all muscle samples ($n = 30$). B: mean SD within each monkey, all samples grouped ($n = 4$). C: mean SD within each muscle group, all monkeys grouped ($n = 6$). D: mean SD within the same muscle group and monkey ($n = 8$). E: mean SD within the same muscle sampled chronically and acutely ($n = 4$). F: mean SD within the same muscle over multiple chronic sessions ($n = 10$).

lis and brachialis from *monkey C;* Fig. 8, D). We also observed no substantial differences in PTD rotation between the few samples recorded by both acute and chronic methods (3.5° SD; Fig. 8, E). Significant differences could be expected if the two methods sampled different motor unit populations that exhibited different PTDs (Herrmann and Flanders 1998; Hoffer et al. 1987; van Zuylen et al. 1988). Last, the between-session variability was assessed by comparing chronic recordings from different days. With five samples from each muscle, we found highly consistent PTDs. The mean angular SD across sessions was 3.5° (Fig. 8, F).

Modeling muscle activation

We tested whether the minimization of various measures of muscular activity—such as summed muscle force ($[sumn]f^n$) (Penrod et al. 1974), muscle metabolic energy $[[sumn](f_i*l_i)^n]$ (Happee 1992), or muscle noise $[[sumn](f_i*/PCSA_i)^n]$ (Hamilton et al. 2004)—would predict PTD rotations similar to the monkey's upper limb muscles. Figure 9 shows the predicted activity of the noise model for each muscle group at the power $n = 2$ (compare with Fig. 6); note that similar predictions were obtained for the other two models. Each muscle group was predicted to have unimodal tuning with a range of tuning widths between muscle groups. Importantly, the noise model predicted PTD rotations toward SE/EF or SF/EE (Fig. 10).
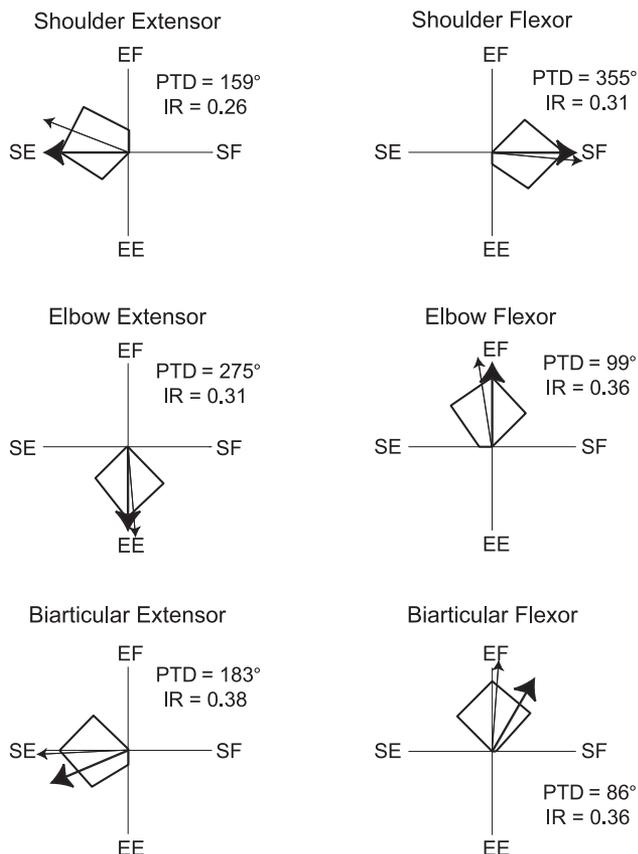

FIG. 9. Predicted muscle activity from the noise model at $n = 2$. Each panel illustrates the models' predicted activity levels (solid lines) over the 8 load conditions for one muscle group. The model's PTD (small arrow) is also compared with the anatomical action of each muscle group (large arrow). All 6 muscle groups are presented: shoulder flexor/extensor, elbow flexor/extensor, and biarticular flexor/extensor.

PTD rotations were apparent for most muscle groups with a large range between muscle groups: (3–26°, noise), (3–16°, force), and (−3–17°, energy; Figs. 9 and 10). We also augmented the model to include all the individual muscles. The augmented model predicted the same PTD rotation for all the muscles within each muscle group. For example, the PTD of all elbow flexors would rotate equally, regardless of their moment arm magnitude, PSCA, and fascicle length.

Exploring the parameters of the muscle models indicated that rotation of the PTDs was robust. For the range of scaling powers tested ($[sumn]f^n$), all models correctly predicted that the monoarticulars' PTDs would rotate toward SE/EF or SF/EE. For powers near 1, all models incorrectly predicted that at least one biarticular would rotate toward flexion/flexion or extension/extension, but for powers near 2 and above, only the energy model continued to incorrectly predicted biarticular rotation. Increasing the scaling power beyond 2 had small and/or inconsistent effects on the magnitude of rotation across muscles although it led to increasingly broader tuning (Fig. 10). It should be noted that all models underestimated the magnitude of observed PTD rotation, did not predict the generally larger PTD rotation for flexors versus extensors, and did not predict PTD rotations on a muscle-group by muscle-group basis.

A sensitivity analysis indicated that the above effects were robust to errors in estimating the moment arms of the biarticulars. Importantly, as long as the biarticulars occupied flexor-flexor and extensor-extensor quadrants then the monoarticulars would rotate toward SE/EF or SF/EE.

DISCUSSION

Summary

In this paper, we report the torque-related activity of primate shoulder and elbow muscles during a postural task where we selectively applied loads only to the shoulder, only to the elbow, or to both joints together (see METHODS). Importantly, the ability to experimentally load each joint independently revealed that the activity of single-joint muscles varies with the torque generated at the adjacent unspanned joint. Monoarticular elbow flexors and shoulder extensors were maximally sensitive to a combination of elbow-flexion and shoulder-extensor torque. In contrast, monoarticular elbow extensors and shoulder flexors were maximally sensitive to a combination of elbow-extensor and shoulder-flexor torque. Biarticular flexor-flexors and extensor-extensors also showed a bias in their preferred torque direction toward shoulder-extension/elbow-flexion. This pattern of PTD rotation was qualitatively reproduced by models that minimize a global measure of muscular activity such a force, metabolic energy, or noise.

Influence of biarticular muscles at the shoulder and elbow joints

The critical factor for PTD rotations of shoulder and elbow muscles is the presence of biarticular muscles. This influence is easily seen in three simple muscle-configurations involving an elbow, shoulder, and biarticular muscle-pair (Fig. 11). Importantly, the different muscle configurations result in different recruitment patterns of the elbow flexor with additional shoulder extensor torque (Fig. 11, *row 1*), shoulder flexor torque

Noise Model

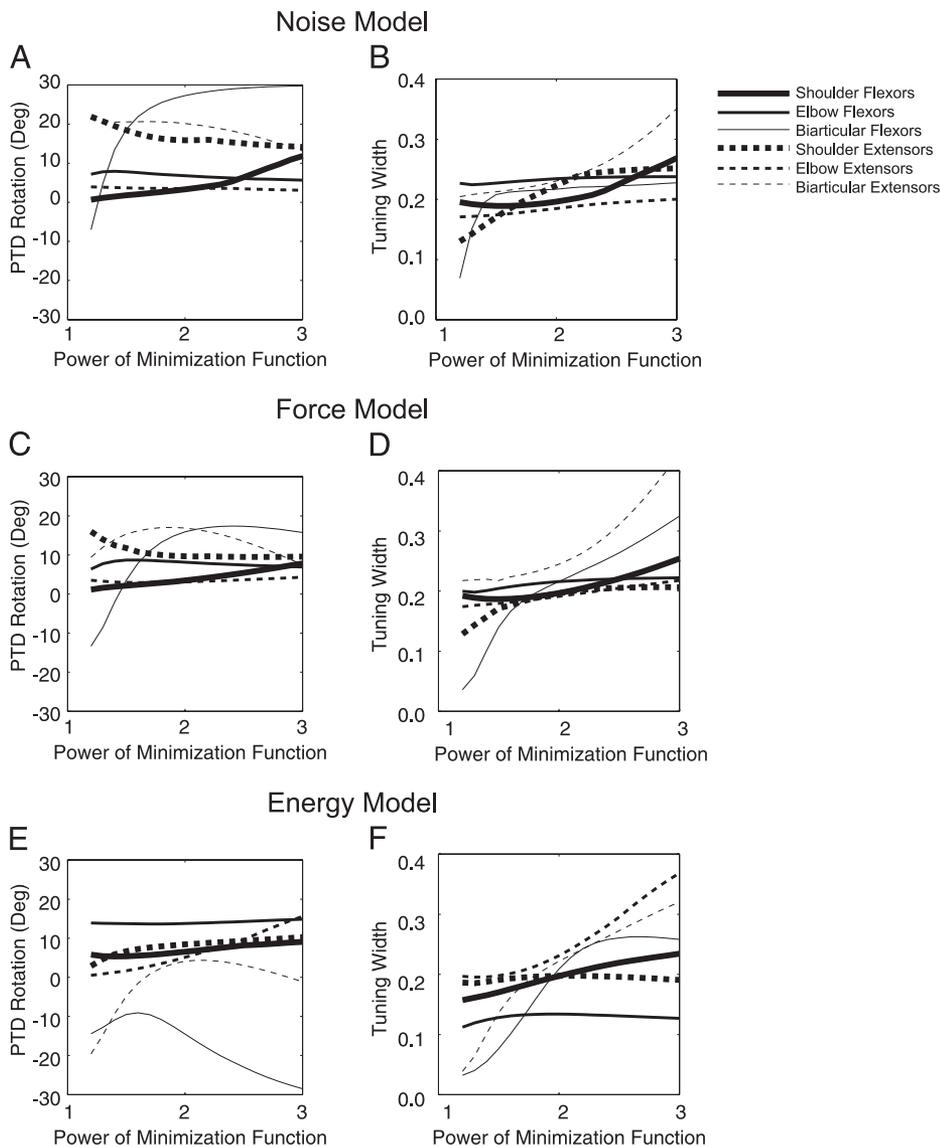## Force Model

Energy Model

FIG. 10. Predicted PTD rotation and tuning width with different scaling powers. *A* and *B*: noise model. *C* and *D*: force model. *E* and *F*: energy model. Solid lines, flexors; dashed lines, extensors; thick lines, shoulder muscles; medium lines, elbow muscles; thin lines, biarticulars.

(*row 3*), or no shoulder torque (*row 2*). For this simple model, all muscle parameters such as PSCA and moment arm are uniform.

The first muscle configuration includes an elbow flexor and shoulder muscle-pair (Fig. 11*A*). Here the elbow muscle is activated by the same amount for the same required elbow torque regardless of the required shoulder torque as no other muscle can produce elbow torque. Thereby, the elbow flexor's PTD is aligned with its anatomical action at 90° (Fig. 11*A, bottom*).

The second muscle configuration includes the elbow flexor and a biarticular muscle pair (Fig. 11*B*). Because the biarticular muscle-pair produces both shoulder and elbow torque, the single-joint elbow flexor must change its level of activity; otherwise, the net elbow flexor torque will be insufficient or excessive. This means that the elbow flexor's PTD will rotate from its anatomical action toward the large gap in torque-space (120°) (Fig. 11*B, bottom*) by the amount that the biarticular-pair is deviated from the shoulder axis (30°). The resulting PTD rotation is trivial insofar as it is the only possible solution.

The first and second muscle configurations are nonredundant because a target torque can be achieved by only one combination of the muscles' activity. In contrast, rotations of PTDs are not necessary in a redundant muscle-configuration where the elbow, shoulder, and biarticulars are all present. Because a redundant muscle configuration can achieve the target torques by an infinite number of muscle combinations, a particular and consistent solution reflects a favored strategy for muscle activation.

In dealing with redundancy one could indirectly specify the muscular activity via a minimizing constraint, "the solution with the lowest X" because there may be only one pattern of muscular activation that both achieves the targeted torque and satisfies the constraint. In the third muscle configuration, Fig. 11*C,* the summed square of "muscle" activity is minimized. This results in a lower activation of the elbow flexor during the elbow torque-only condition than occurs with the two nonredundant systems. Biarticular activation also leads to larger elbow flexor activation with additional shoulder extensor torque, i.e., the elbow flexor's PTD is rotated toward the largest
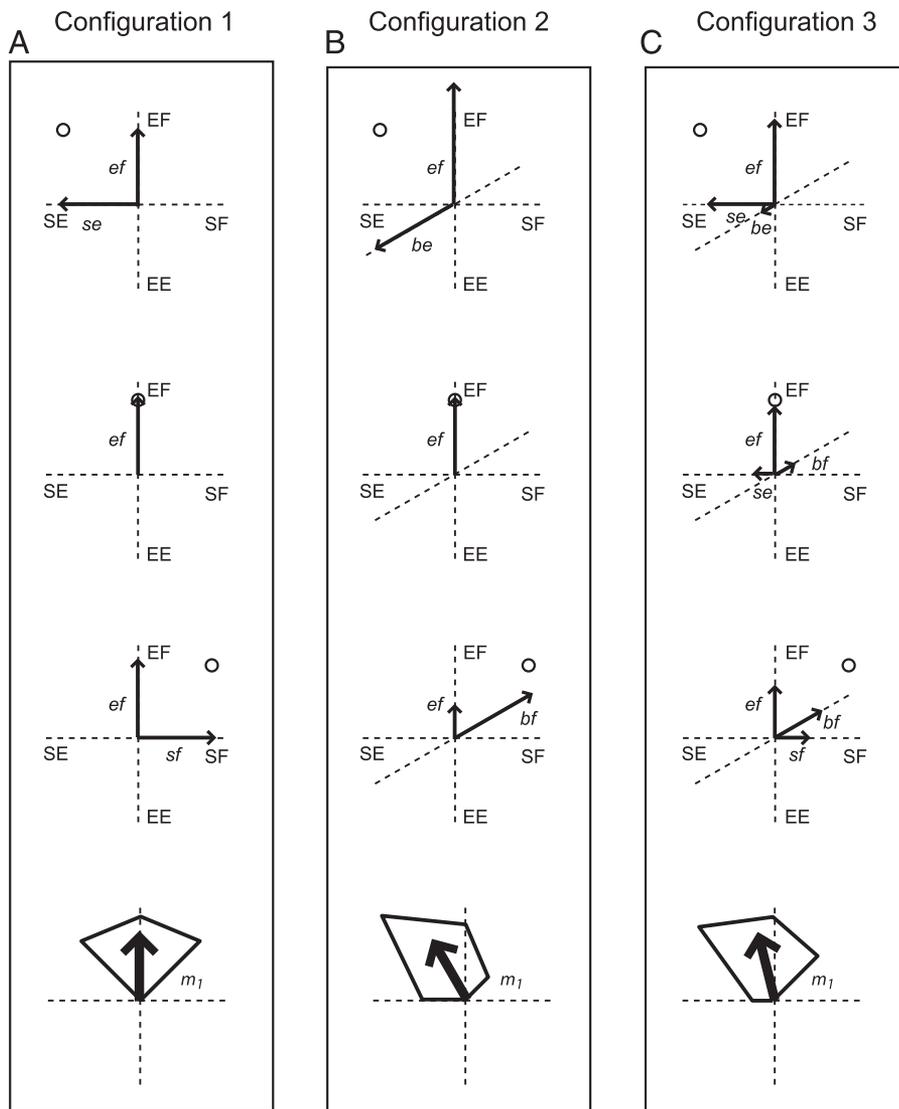
FIG. 11. Influence of muscle configuration on muscle activity. Three simple muscle configurations (*A—C*) produced a target torque (open circle) involving a fixed level of elbow flexor torque paired with extensor (*row 1*), flexor (*row 3*), or no torque (*row 2*) at the shoulder. Torque is indicated by upper case symbols and muscle activation is indicated by lower case. *Bottom row*: the monoarticular elbow flexor activity for each target torque and the respective PTD. *A*: orthogonal, nonredundant muscle configuration consisting of only monoarticular muscles. *B*: nonorthogonal, nonredundant muscle configuration where monoarticular and biarticular muscles are activated alone or in pairs. *C*: nonorthogonal, nonredundant muscle configuration (reminiscent of the upper limb) where monoarticular and biarticular muscles can be activated in any combination.

gap (Fig. 11*C, bottom*). Last, the shoulder extensor is activated during the elbow-torque only condition to counter biarticular's shoulder flexor torque such that its PTD is biased toward the same shoulder/elbow quadrant as the elbow flexor.

The results of this simple model demonstrate that minimization of activity-related measures lead to rotations of the monoarticulars' PTDs toward the largest gaps in torque-space (see also Fagg et al. 2002; Nozaki et al. 2005). Biarticular muscles of the primate upper limb act in the quadrants for extension/extension and flexion/flexion. Consequently, monoarticular PTD rotations toward the opposite quadrants involving extension at one joint and flexion at the other lead to a reduction of total muscular activity and effects of motor noise, similar to what is observed. [Similar PTD rotations can occur at a single joint having multiple degrees of freedom when the spanning muscles are unevenly distributed (Fagg et al. 2002; Hoffman and Strick 1999).]

Muscle activation models

It should be emphasized that identical minimization models have been previously employed to examine recruitment order, degree of

activation, and tuning width of muscles (Crowninshield and Brand 1981; Dul et al. 1984; Jongen et al. 1989a; Penrod et al. 1974; van Bolhuis and Gielen 1999). The rotation of PTDs from their anatomical action has been less frequently examined (Fagg et al. 2002; Nozaki et al. 2005; van Zuylen et al. 1988). Our experimental and modeling effort provides an addition to the latter.

Testing among the three models requires considering their physiological plausibility and accuracy. As per physiological plausibility, there are sufficient peripheral and central pathways to represent either metabolic energy, muscle force, or muscle noise (Gandevia 2001; Hulliger 1984; Jami 1992; McCloskey 1981; Mense 1996). In terms of accuracy, all models accounted for rotations of the monoarticular PTDs throughout the parameter space. When the models were raised to a power near 1, they all incorrectly predicted the rotation direction for at least one biarticular, but only the metabolic energy model continued to incorrectly predict biarticular rotation raised to a power near and >2. Thereby we consider the metabolic energy model to be the least likely as well as other models raised to a power near 1. We could find no empirical feature to unambiguously choose between the force and noise models.

These conclusions are consistent with the earlier work by van Bolhuis and Gielen (1999) on human arm muscle activity when countering endpoint loads. Instead of PTD rotations they examined changes in tuning width and the general orientation of activation with different limb configurations compared with the force, energy, and noise models mentioned; note that PTD rotations are apparent though they were not reported in their study. The energy model and any cost functions raised to $n = 1$ or $n = 3$ were rejected as incorrectly predicting a large influence of limb configuration on elbow muscle activation and too narrow tuning and too broad tuning, respectively. The authors conclude that the force and noise models with $n = 2$ were the best candidates.

Several limitations of our data preclude a more detailed assessment of the models including the high variability of rotation magnitude (see RESULTS) and tuning width. For example, muscle depth likely influences EMG responses. Greater activity and broader tuning would be expected deeper within a muscle where slow fibers with lower thresholds predominate compared with more superficial regions with predominantly fast fibers that show minimal activity for low-level contractions (Henneman 1957; Singh et al. 2002). Likewise, previous studies have demonstrated that the different motor units that comprise a muscle can exhibit different preferred directions (Herrmann and Flanders 1998; Hoffer et al. 1987; Jongen et al. 1989b; van Zuylen et al. 1988;). Consequently, some of this variability in tuning width and PTDs may reflect actual differences within a single muscle or between muscles (see *Deviations of PTD from the anatomical action*, Fig. 3*B*). Last, we did not monitor torques about all the arm's degrees of freedom such as shoulder abduction/adduction and shoulder internal/external rotation. We expect such torques would be quite small due to their inefficiency within a simple and highly-practiced task, but such torques could vary in subtle ways across different loads or sessions leading to variability in PTDs. Determining the relative contribution of these possibilities will require sampling from a more uniform muscle population, imposing more load conditions, and controlling for all the torques about the shoulder.

It should be noted that the mathematical models predict that, regardless of the minimization variable and coefficient magnitude, each muscle group has a unique tuning width and rotation of PTD (see Fig. 10). Therefore the present results suggest that a fixed tuning width and rotation magnitude will likely not occur for nonorthogonal and redundant muscle organizations that employ a minimizing recruitment strategy.

Implications for muscle "synergies"

The present results could be described by two explicit grouping of multiple muscles into a functional unit—SE/EF and SF/EE. Such synergies are appealing as they would allow the motor system to achieve flexible motor programming while reducing the neuromuscular degrees of freedom (Bernstein 1967; d'Avella et al. 2003; Ivanenko et al. 2004; MacPherson et al. 1986; Ting and MacPherson 2005; Tresch et al. 1999). However, a qualitatively similar pattern was achieved without specifying any synergies but by minimizing a global cost of activity.

Minimizing the activity of a nonorthogonal and redundant muscle system can lead to surprising results. We observed that anterior deltoid—a single-joint muscle—responded almost equally to shoulder and elbow loads, whereas biceps brachii—a biarticular muscle—responded almost entirely to elbow loads (Fig. 6, Table 1). Muscles with positively correlated anatomical actions—biceps and anterior deltoid; triceps long and triceps lateral—can exhibit negatively correlated functional associations and vice versa (Fig. 6, Table 1). Moreover, muscles with similar moment arm directions (brachialis and brachioradialis; pectoralis major and anterior deltoid; lateral triceps and medial triceps) will exhibit similar PTD rotations despite their widely differing absolute force capabilities—the physiological cross sectional areas varied by a factor of seven (Table 1). Because these features were reproduced without any synergies, patterned co-variation does not require or establish muscle synergies.

Implications for interpreting primary motor cortical activity

Primary motor cortex (M1) is the principle cortical region supporting voluntary motor execution. M1 provides the largest contribution to the corticospinal tract (Dum and Strick 1991), a dense descending projection forming multi-muscle linkages largely through spinal interneurons but also through direct synaptic connections with motoneurons (Fetz and Cheney 1987; Lemon and Griffiths 2005). Individual M1 neurons also discharge with the rate, direction, magnitude and onset of muscular output (Ashe 1997; Evarts 1968; Fetz and Cheney 1987; Holdefer and Miller 2002; Porter and Lemon 1993; Scott 2003; Sergio and Kalaska 2003; Todorov 2000).

The activity patterns of proximal limb muscles and the associated minimization models of the musculoskeletal system provide an important basis for interpreting neural responses in M1. It may seem reasonable to assume that neurons that respond to variations in muscular torque at both joints exert control over muscles at both joints. But this assumption is clearly incorrect because virtually all monoarticulars respond to loads at both joints. Second, the bias in the distribution of PTDs of M1 neurons during the postural task (Cabel et al. 2001) could suggest it possesses a predominant representation of multi-joint synergies for whole-limb flexors (shoulder extensors-elbow flexors) and whole-limb extensors (shoulder flexors-elbow extensors) over the opposing combinations of muscles. As stated earlier for interpreting muscle activities, optimization models with no explicit muscle groupings create similar patterns of muscle activity, suggesting that the observed distribution of PTDs in M1 is not necessarily a neural representation of muscle synergies.

The parallel between the results of optimization models and M1 activity likely reflects a fundamental aspect of M1 function, specifically, and the entire motor system, generally. Objective functions such as minimizing muscle noise provide an ethologically compelling link between behavioral goals and patterns of muscle activity (Harris and Wolpert 1998). The present results are consistent with the idea that M1 forms a key component of a motor system designed to make this conversion of global goals into patterns of muscle activity (Scott 2004). Thus the bias in the distribution of PTDs in M1 may not be just a reflection of the motor periphery but also a reflection of an optimization process performed by the sensorimotor system.

REFERENCES

Ashe J. Force and the motor cortex. *Behav Brain Res* 87: 255–269, 1997.

Batschelet E. *Circular Statistics in Biology.* New York: Academic, 1981.

Bernstein NA. *The Coordination and Regulation of Movements.* Oxford, UK: Pergamon, 1967.

Buchanan TS, Almdale DP, Lewis JL, and Rymer WZ. Characteristics of synergic relations during isometric contractions of human elbow muscles. *J Neurophysiol* 56: 1225–1241, 1986.

Buchanan TS, Rovai GP, and Rymer WZ. Strategies for muscle activation during isometric torque generation at the human elbow. *J Neurophysiol* 62: 1201–1212, 1989.

Cabel DW, Cisek P, and Scott SH. Neural activity in primary motor cortex related to mechanical loads applied to the shoulder and elbow during a postural task. *J Neurophysiol* 86: 2102–2108, 2001.

Canedo A. Primary motor cortex influences on the descending and ascending systems. *Prog Neurobiol* 51: 287–335, 1997.

Cheng EJ and Scott SH. Morphometry of *Macaca mulatta* forelimb. I. Shoulder and elbow muscles and segment inertial parameters. *J Morphol* 245: 206–224, 2000.

Crowninshield RD and Brand RA. A physiologically based criterion of muscle force prediction in locomotion. *J Biomech* 14: 793–801, 1981.

d'Avella A, Saltiel P, and Bizzi E. Combinations of muscle synergies in the construction of a natural motor behavior. *Nat Neurosci* 6: 300–308, 2003.

Dul J, Johnson GE, Shiavi R, and Townsend MA. Muscular synergism. II. A minimum-fatigue criterion for load sharing between synergistic muscles. *J Biomech* 17: 675–684, 1984.

Dum RP and Strick PL. The origin of corticospinal projections from the premotor areas in the frontal lobe. *J Neurosci* 11: 667–689, 1991.

Evarts EV. Relation of pyramidal tract activity to force exerted during voluntary movement. *J Neurophysiol* 31: 14–27, 1968.

Fagg AH, Shah A, and Barto AG. A computational model of muscle recruitment for wrist movements. *J Neurophysiol* 88: 3348–3358, 2002.

Fetz EE and Cheney PD. Functional relations between primate motor cortex cells and muscles: fixed and flexible. *Ciba Found Symp* 132: 98–117, 1987.

Gandevia SC. Spinal and supraspinal factors in human muscle fatigue. *Physiol Rev* 81: 1725–1789, 2001.

Graham KM, Moore KD, Cabel DW, Gribble PL, Cisek P, and Scott SH. Kinematics and kinetics of multijoint reaching in nonhuman primates. *J Neurophysiol* 89: 2667–2677, 2003.

Graham KM and Scott SH. Morphometry of Macaca mulatta forelimb. III. Moment arm of shoulder and elbow muscles. *J Morphol* 255: 301–314, 2003.

Gribble PL and Scott SH. Method for assessing directional characteristics of non-uniformly sampled neural activity. *J Neurosci Methods* 113: 187–197, 2002.

Hamilton AF, Jones KE, and Wolpert DM. The scaling of motor noise with muscle strength and motor unit number in humans. *Exp Brain Res* 157: 417–430, 2004.

Happee R. *The Control of Shoulder Muscles During Goal Directed Movements* (PhD dissertation). Delft, The Netherlands: Delft University of Technology, 1992.

Harris CM and Wolpert DM. Signal-dependent noise determines motor planning. *Nature* 394: 780–784, 1998.

Henneman E. Relation between size of neurons and their susceptibility to discharge. 417. *Science* 126: 1345–1347, 1957.

Hepp-Reymond M. Functional organization of motor cortexand its participation in voluntary movements. In: *Comparative Primate Biology,* edited by Alan R. New York: Liss, 1988, p. 501–624.

Herrmann U and Flanders M. Directional tuning of single motor units. *J Neurosci* 18: 8402–8416, 1998.

Hoffer JA, Loeb GE, Sugano N, Marks WB, O'Donovan MJ, and Pratt CA. Cat hindlimb motoneurons during locomotion. III. Functional segregation in sartorius 55. *J Neurophysiol* 57: 554–562, 1987.

Hoffman DS and Strick PL. Step-tracking movements of the wrist. IV. Muscle activity associated with movements in different directions. *J Neurophysiol* 81: 319–333, 1999.

Holdefer RN and Miller LE. Primary motor cortical neurons encode functional muscle synergies. *Exp Brain Res* 146: 233–243, 2002.

Hulliger M. The mammalian muscle spindle and its central control. *Rev Physiol Biochem Pharmacol* 101: 1–110, 1984.

Ivanenko YP, Poppele RE, and Lacquaniti F. Five basic muscle activation patterns account for muscle activity during human locomotion. *J Physiol* 556: 267–282, 2004.

Jami L. Golgi tendon organs in mammalian skeletal muscle: functional properties and central actions. *Physiol Rev* 72: 623–666, 1992.

Jongen HA, Denier van der Gon JJ, and Gielen CC. Activation of human arm muscles during flexion/extension and supination/pronation tasks: a theory on muscle coordination. *Biol Cybern* 61: 1–9, 1989a.

Jongen HA, Denier van der Gon JJ, and Gielen CC. Inhomogeneous activation of motoneurone pools as revealed by co-contraction of antagonistic human arm muscles. *Exp Brain Res* 75: 555–562, 1989b.

Kurtzer I, Herter TM, and Scott SH. Random change in cortical load representation suggests distinct control of posture and movement. *Nat Neurosci* 8: 498–504, 2005.

Lemon RN and Griffiths J. Comparing the function of the corticospinal system in different species: organizational differences for motor specialization? *Muscle Nerve* 2005.

Loeb GE and Gans C. *Electromyography for Experimentalists,* London: University of Chicago Press, 1983.

Macpherson JM, Rushmer DS, and Dunbar DC. Postural responses in the cat to unexpected rotations of the supporting surface: evidence for a centrally generated synergic organization. *Exp Brain Res* 62: 152–160, 1986.

McCloskey DI. Corollary discharges: motor commands and perception. In: *Handbook of Physiology. The Nervous System. Motor Control.* Washington, DC: Am. Physiol. Soc., 1981, vol. II, p. 1415–1447.

Mense S. Group III and IV receptors in skeletal muscle: are they specific or polymodal? 49. *Prog Brain Res* 113: 83–100, 1996.

Nozaki D, Nakazawa K, and Akai M. Muscle activity determined by cosine tuning with a nontrivial preferred direction during isometric force exertion by lower limb. *J Neurophysiol* 93: 2614–2624, 2005.

Osu R and Gomi H. Multijoint muscle regulation mechanisms examined by measured human arm stiffness and EMG signals. *J Neurophysiol* 81: 1458–1468, 1999.

Penrod DD, Davy DT, and Singh DP. An optimization approach to tendon force analysis. *J Biomech* 7: 123–129, 1974.

Porter R and Lemon RN. *Corticospinal Function and Voluntary Movement.* New York: Oxford, 1993.

Sanes JN and Donoghue JP. Plasticity and primary motor cortex. *Annu Rev Neurosci* 23: 393–415, 2000.

Scott SH. Apparatus for measuring and perturbing shoulder and elbow joint positions and torques during reaching. *J Neurosci Methods* 89: 119–127, 1999.

Scott SH. The role of primary motor cortex in goal-directed movements: insights from neurophysiological studies on non-human primates. *Curr Opin Neurobiol* 13: 671–677, 2003.

Scott SH. Optimal feedback control and the neural basis of volitional motor control. *Nat Rev Neurosci* 5: 532–546, 2004.

Scott SH and Kalaska JF. Reaching movements with similar hand paths but different arm orientations. I. Activity of individual cells in motor cortex. *J Neurophysiol* 77: 826–852, 1997.

Sergio LE and Kalaska JF. Systematic changes in motor cortex cell activity with arm posture during directional isometric force generation. *J Neurophysiol* 89: 212–228, 2003.

Singh K, Melis EH, Richmond FJ, and Scott SH. Morphometry of *Macaca mulatta* forelimb. II. Fiber-type composition in shoulder and elbow muscle. *J Morphol* 251: 323–332, 2002.

Soechting JF and Lacquaniti F. Quantitative evaluation of the electromyographic responses to multidirectional load perturbations of the human arm. *J Neurophysiol* 59: 1296–1313, 1988.

Theeuwen M, Gielen CC, Miller LE, and Doorenbosch C. The relation between the direction dependence of electromyographic amplitude and motor unit recruitment thresholds during isometric contractions. *Exp Brain Res* 98: 488–500, 1994.

Ting LH and Macpherson JM. A limited set of muscle synergies for force control during a postural task. *J Neurophysiol* 93: 609–613, 2005.

Todorov E. Direct cortical control of muscle activation in voluntary arm movements: a model. *Nat Neurosci* 3: 391–398, 2000.

Todorov E and Jordan MI. Optimal feedback control as a theory of motor coordination. *Nat Neurosci* 5: 1226–1235, 2002.

Tresch MC, Saltiel P, and Bizzi E. The construction of movement by the spinal cord. *Nat Neurosci* 2: 162–167, 1999.

van Bolhuis BM and Gielen CC. A comparison of models explaining muscle activation patterns for isometric contractions. *Biol Cybern* 81: 249–261, 1999.

van Zuylen EJ, Gielen CC, and Denier van der Gon JJ. Coordination and inhomogeneous activation of human arm muscles during isometric torques. *J Neurophysiol* 60: 1523–1548, 1988.